

## Phonon-Mediated Coupling of InGaAs/GaAs Quantum-Dot Excitons to Photonic Crystal Cavities

M. Calic,<sup>1,\*</sup> P. Gallo,<sup>1</sup> M. Felici,<sup>1,†</sup> K. A. Atlasov,<sup>1</sup> B. Dwir,<sup>1</sup> A. Rudra,<sup>1</sup> G. Biasiol,<sup>2</sup> L. Sorba,<sup>3</sup>  
G. Tarel,<sup>4</sup> V. Savona,<sup>4</sup> and E. Kapon<sup>1</sup>

<sup>1</sup>Laboratory of Physics of Nanostructures, Ecole Polytechnique Fédérale de Lausanne (EPFL), CH-1015 Lausanne, Switzerland

<sup>2</sup>Istituto Officina dei Materiali CNR, Laboratorio TASC, I-34149 Trieste, Italy

<sup>3</sup>NEST, Istituto Nanoscienze-CNR and Scuola Normale Superiore, I-56126 Pisa, Italy

<sup>4</sup>Institut de Théorie des Phénomènes Physiques, Ecole Polytechnique Fédérale de Lausanne (EPFL), CH-1015 Lausanne, Switzerland

(Received 1 March 2011; published 1 June 2011)

We demonstrate that the emission characteristics of site-controlled InGaAs/GaAs single quantum dots embedded in photonic crystal slab cavities correspond to single confined excitons coupled to cavity modes, unlike previous reports of similar systems based on self-assembled quantum dots. By using polarization-resolved photoluminescence spectroscopy at different temperatures and a theoretical model, we show that the exciton-cavity interaction range is limited to the phonon sidebands. Photon-correlation and pump-power dependence experiments under nonresonant excitation conditions further establish that the cavity is fed only by a single exciton.

DOI: 10.1103/PhysRevLett.106.227402

PACS numbers: 78.67.Hc, 42.50.Pq, 42.70.Qs, 78.55.Cr

The coupling between confined excitons in semiconductor quantum dots (QDs) and photons trapped in nanocavities can be an important resource in the context of quantum information [1]. Owing to recent research efforts in the field of cavity quantum electrodynamics in the solid state, important milestones were achieved in the realization and study of single QD-cavity systems, culminating in reported demonstrations of striking phenomena such as vacuum Rabi splitting [2–5], laser oscillation [6], and photon blockade [7]. However, there are several problems inherent to the self-assembled QDs (SAQDs) that are customarily used in these experiments. First, the random nature of the QD nucleation process makes it very challenging to control both the position and the spectral properties of the dots [8], so that a scalable approach towards device implementation becomes undermined [9]. Second, SAQDs show unexpected far off-resonance (FOR) exciton-cavity coupling for detunings much greater than the mode linewidth [10–17]. This feature is a major departure from the ideal picture of a two-level system interacting with a cavity mode, which severely limits applications in cavity quantum electrodynamics.

Different processes have been proposed for explaining light emission from a nonresonant cavity. First, QD excitons inevitably interact with their semiconductor environment via the emission or absorption of thermally activated acoustic phonons [18] or due to randomly trapped charges in the vicinity of the QD [19]. These dephasing processes are known to broaden the line shape of QD transitions and to facilitate QD-cavity coupling beyond a detuning interval defined purely by the lifetime-limited QD transition [20–22]. However, exciton-phonon interactions and pure dephasing mechanisms can only explain dot-cavity coupling within a detuning range of a few meV. Second, it was

demonstrated that the higher excited states in SAQDs hybridize with the neighboring wetting layer states, forming a continuum of multiexcitonic transitions, which translates into a broad background visible in photoluminescence (PL) spectra [12,23]. When a SAQD is placed inside a nanocavity, the continuum-associated transitions can become strongly enhanced through the Purcell effect, thereby facilitating light emission from a cavity mode (CM) even if it is detuned by  $> \pm 10$  meV from the discrete QD spectral features. The latter mechanism has been identified to be at the origin of the FOR coupling observed in a series of recent studies [10–17]. FOR coupling was successfully suppressed by means of an applied electric field [14] or by exploiting resonant excitation [15]. However, the former measure leads to a dramatic increase in spin relaxation through the Rashba effect [24], while the latter is impractical for applications where electrical pumping is required. In this Letter, we demonstrate the absence of FOR coupling in the case of site-controlled pyramidal QDs (PQDs) [25] integrated with photonic crystal (PhC) defect cavities. Our findings suggest that PQDs couple through truly 3D-confined excitonic states, such that the wave function overlap between localized QD states and barrier states is negligible and thus the origin of FOR coupling is eliminated.

The fabrication of the PQD-cavity structures consists of metal-organic vapor phase epitaxy of InGaAs/GaAs QDs on (111)B GaAs substrates patterned with inverted pyramids and subsequent processing of PhC membrane structures aligned with the PQDs (see Ref. [26]). While SAQDs and site-controlled versions thereof [8] rely on a strain-induced formation of QDs on top of a 2D wetting layer, the growth processes leading to QD nucleation in the case of PQDs are essentially determined by an interplay between

growth rate anisotropy and nanocapillarity effects [27]. Taking advantage of the improved QD uniformity and optical quality, and of the better control over the emission wavelength obtained by using dense pyramid patterns (inhomogeneous broadening 1 meV, exciton linewidth 100  $\mu\text{eV}$ ) [27,28], we based the fabrication of our structures on PQD arrays of 400 nm pitch [Fig. 1(a)]. By using an optimized  $L3$  cavity design, all PQDs except for the one in the center of the cavity are etched away [Fig. 1(b)]. We verified by means of a secondary electron microscope that the mutual alignment accuracy between the PQD arrays and the PhC hole patterns was 50 nm across the whole substrate [see the example in Fig. 1(c)]. As evidenced by the 3D finite difference time domain simulation of the confined optical field shown in Fig. 1(d), this precision is sufficient for positioning the PQD at a point where the intensity is at least 60% of its maximum value for the fundamental cavity mode. By using this fabrication approach, we were able to obtain QD-cavity structures with spectra showing distinct coupling [Fig. 1(e)] in a deterministic and reproducible fashion. The measured quality ( $Q$ )

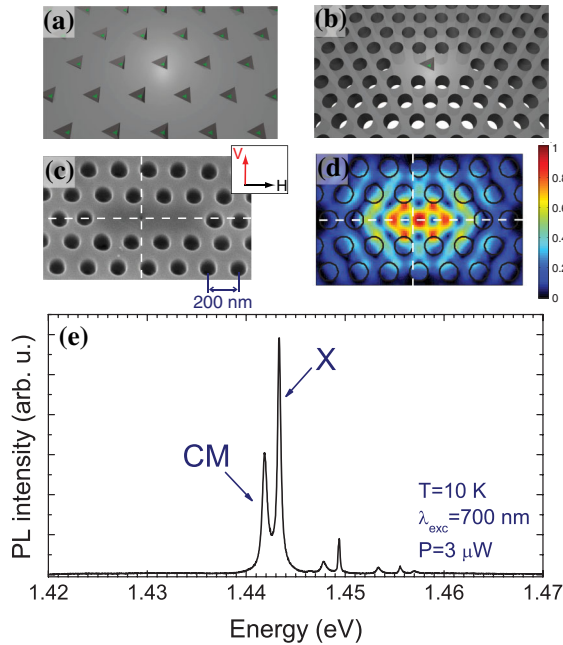


FIG. 1 (color online). (a) Schematic illustration of a hexagonal array of pyramidal recesses, each with a side length of  $\sim 300$  nm and containing a single PQD (green dots). (b) A PhC structure coaligned with the underlying PQD array with a lattice constant equal to half the pyramid pitch defines the single QD nanocavity system. (c) Secondary electron microscope image of an actual structure (slightly tilted perspective), with the location of the QD marked by the crossing of the dashed lines. (d) Spatial distribution of the electric field intensity of the fundamental cavity mode, computed by 3D finite difference time domain simulation. This mode is mainly polarized along the  $V$  axis indicated in (c). (e) PL spectrum of a typical PQD-cavity structure showing the exciton emission ( $X$ ) and the fundamental CM.

factors were rather moderate [ $Q \sim 2500$  in Fig. 1(e)], which is probably due to PhC disorder and residual absorption by bulk and surface states in the membrane layer. However, such  $Q$  values are well suited for observing and studying the dot-cavity coupling mechanism addressed here.

A first indication of the short-ranged nature of the coupling of PQDs to PhC cavities can be deduced from the PL spectra presented in Figs. 2(a) and 2(b), where the emission was resolved in linear polarization along the  $H$  and  $V$  directions [as defined in Fig. 1(c)]. Results for two nominally identical PQD-cavity structures (called  $A$  and  $B$  here) are presented here to show the reproducibility of our data. For structure  $A$ , at 10 K an exciton ( $X$ ) feature is observed at 1.5 meV detuning with respect to a strongly  $y$ -polarized CM. As the  $X$  is tuned into resonance with the CM by raising the temperature, the former becomes increasingly copolarized with the cavity mode. At higher temperatures ( $> 50$  K), the  $X$  emission feature eventually recovers its initial polarization state. A similar behavior is evident for the PQD-cavity structure  $B$ , as shown in Fig. 2(b). These observations suggest a dot-cavity coupling mechanism that is effective only within a small detuning range. By using the degree of linear polarization  $\sigma = \frac{I_V - I_H}{I_H + I_V}$ , where  $I_H$  and  $I_V$  stand for the integrated intensity components,

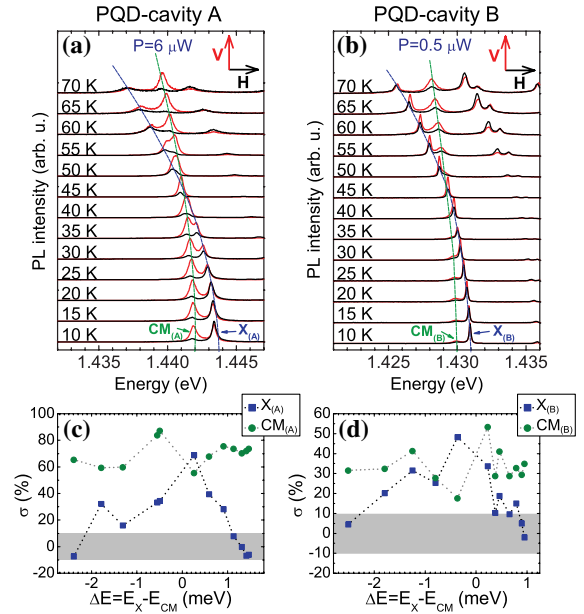


FIG. 2 (color online). Polarization-resolved photoluminescence measurements. (a),(b) Temperature scanning of the dot-cavity detuning for two different PQD-cavity structures. (c), (d) Degree of polarization  $\sigma$  versus detuning of the  $X$  and CM lines for the two samples. The dashed lines are guides to the eye. The gray-shaded area in (c) and (d) depicts the typical range for  $\sigma$  in the case of bare PQDs (i.e., dots that were not incorporated in a cavity structure). In both (a) and (b), the structures were nonresonantly excited with  $\lambda_{\text{exc}} = 700$  nm.

respectively, along  $H$  and  $V$ , we summarize the evolution of the polarization features of the  $X$  and the CM lines in Figs. 2(c) and 2(d). For both PQD-cavity systems, the trend of  $\sigma$  reveals that the presence of the CM alters the polarization of the  $X$  emission of a PQD only within a small detuning range of  $\sim 2$  meV, thereby strongly hinting at the absence of FOR coupling. On the contrary, in similar experiments involving SAQDs, the QD features were found to be strongly copolarized to a nearby CM line despite an energy mismatch of  $\Delta E = E_X - E_{CM} \approx +4$  meV [29].

The spectral range of exciton-mode coupling also manifests itself in the corresponding second-order photon-correlation function  $g^{(2)}(\tau)$ , where  $\tau$  refers to the delay between two photon detection events. Figure 3(a) shows the measured correlation histograms acquired for the  $X$  and CM lines of PQD-cavity system  $A$  at 10 K ( $\Delta E \approx +1.5$  meV). The antibunching observed in the  $X$ - $X$  and CM-CM autocorrelations, as well as in the CM- $X$  cross correlation, unambiguously proves that the coupling between the PQD and the cavity mode is regulated at the level of single photons and that also the cavity emission takes place in the quantum regime. Previous reports of similar experiments, but with SAQDs, revealed that the photons emitted by the cavity exhibited classical correlations (or an unexpected bunching), which is an artifact originating from FOR coupling occurring in that case [10,12]. Furthermore, the excitation power dependence in Fig. 3(b) shows that the PL intensities of the  $X$  and CM features increase almost linearly and saturate at the

same power level. This again attests to the absence of contributions from of a multiexcitonic background continuum, which would yield a superlinear power dependence of the cavity emission [12,16].

Our experimental results demonstrate the insignificance of FOR coupling in the emission dynamics of PQDs in nanocavities and suggest that the relevant QD transitions in our case originate solely from QD-confined exciton states rather than hybridized states extending to the barriers surrounding the dots. This is expected for PQDs of the geometry considered here, as evidenced by the quenching of emission from barrier states for pyramidal recesses of size 300 nm [27]. In fact, in this regime, the nanostructures formed on the pyramid facets reduce to extremely thin layers due to nanocapillarity fluxes and possibly degenerate into localized spots, which significantly reduces the overlap between the carrier wave functions confined in the dot and those confined in the lateral barriers. Evidently, dephasing processes that are intrinsic to the semiconductor environment need to be accounted for and should be dominant in the absence of barrier-state hybridization. Recent studies have highlighted the role of phonons in short-range dot-cavity coupling [15,21,30]. Following the theoretical approach of Ref. [20], we modeled the response of our systems by taking into account a nonperturbative interaction between the QD and an acoustic phonon reservoir. The model reproduces the temperature-dependent sidebands that are typically observed in a QD spectrum [18] and predicts enhanced cavity emission for dot-cavity detunings of up to a few meV. Specifically, the modified QD emission spectrum reads

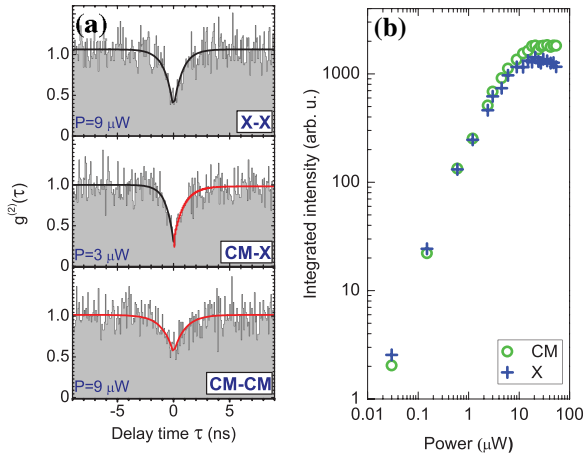


FIG. 3 (color online). Photon-correlation spectroscopy and power dependence measured at  $T = 10$  K ( $\Delta E \approx +1.5$  meV) under nonresonant excitation conditions ( $\lambda_{\text{exc}} = 700$  nm). (a) Second-order photon-correlation histograms for PQD-cavity structure  $A$ . Autocorrelation for the QD exciton (top), cross correlation between the cavity mode and the QD exciton (middle), and autocorrelation of the cavity mode photons (bottom). The black and red lines are exponential fits to the data. (b) Power dependence of the integrated PL for the PQD-cavity structure  $A$ .

$$S(\omega) = \left| \frac{\sqrt{4g^2 - \frac{(\gamma - \kappa)^2}{4}} \left( \omega_c - \omega - i\frac{\kappa}{2} \right)}{\left( \omega_0 - \omega - i\frac{\gamma}{2} + \Sigma(\omega) \right) \left( \omega_c - \omega - i\frac{\kappa}{2} \right) - g^2} \right|^2,$$

where  $g$ ,  $\gamma$ , and  $\kappa$  represent the coupling strength, the exciton free decay rate, and the cavity damping rate, respectively. In this expression, the imaginary part of the exciton-phonon self-energy  $\Sigma(\omega)$  contributes to the QD linewidth. By using this approach, we computed the emission spectra for our PQD-cavity structures  $A$  and  $B$  at two different temperatures. As can be verified in Fig. 4, the theoretical modeling nicely reproduces the measured line shape in both cases. In addition, the model predicts a linear increase of the spectral intensities as a function of excitation power, which we observed experimentally in Fig. 3(b). Thus, we conclude that, in the case of PQDs, the exciton-cavity coupling is dominated by phonon-mediated transitions. Other dephasing mechanisms such as spectral diffusion [19,22] were taken into account phenomenologically as a constant factor in the modeling, by setting  $\gamma$  to match the observed line shape in the PL spectrum.

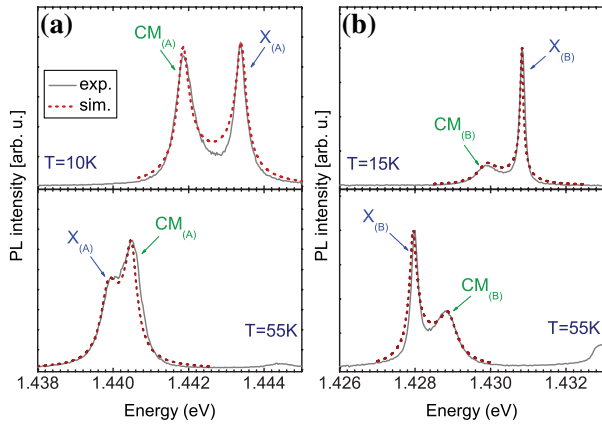


FIG. 4 (color online). Theoretical modeling of phonon-mediated dot-cavity coupling. (a),(b) Computed (dashed lines) and measured (continuous lines) line shapes for the cavity-PQD structure A (a) and B (b). The parameters used in the model are (A)  $g = 150 \mu\text{eV}$ ,  $\gamma = 200 \mu\text{eV}$ , and  $\kappa = 250 \mu\text{eV}$  and (B)  $g = 200 \mu\text{eV}$ ,  $\gamma = 100 \mu\text{eV}$ , and  $\kappa = 250 \mu\text{eV}$ .

In conclusion, FOR coupling is not a universal phenomenon governing the coupling in QD-cavity devices. As we have demonstrated here, QDs with a proper barrier structure do indeed behave like artificial atoms in the solid state, and taking into account the inevitable phonon interactions is sufficient to explain the experimental results rather precisely. Moreover, by using site-controlled QDs, one can rule out the possibility of having other unwanted QDs that overlap with the confined optical mode. The finite (few meV) detuning permitting exciton-cavity coupling mediated by acoustic phonon exchange implies that QD emission via cavity photons can be obtained for a QD spectral distribution of the same magnitude. In this respect, site-controlled PQDs are interesting candidates for the realization of advanced cavity quantum electrodynamics systems [31,32] in view of their demonstrated 1 meV inhomogeneous broadening [28], the possibility to precisely determine their position and to finely adjust their emission energy [27], and their high symmetry, resulting in a vanishing fine structure splitting and in the reproducible generation of polarization-entangled photons [33].

We thank A. Auffèves for fruitful discussions and J. Delgado for assistance with sample characterization.

This work was supported by the Swiss National Science Foundation.

*Note added in proof.*—We very recently became aware that another related work was published [34].

\*milan.calic@epfl.ch

†Present address: Dipartimento di Fisica, Sapienza Università di Roma, P.le A. Moro 2, 00185 Rome, Italy.

- [1] J. L. O'Brien, A. Furusawa, and J. Vuckovic, *Nat. Photon.* **3**, 687 (2009).
- [2] J. P. Reithmaier *et al.*, *Nature (London)* **432**, 197 (2004).
- [3] T. Yoshie *et al.*, *Nature (London)* **432**, 200 (2004).
- [4] E. Peter *et al.*, *Phys. Rev. Lett.* **95**, 067401 (2005).
- [5] G. Khitrova *et al.*, *Nature Phys.* **2**, 81 (2006).
- [6] M. Nomura *et al.*, *Nature Phys.* **6**, 279 (2010).
- [7] A. Faraon *et al.*, *Nature Phys.* **4**, 859 (2008).
- [8] C. Schneider *et al.*, *Nanotechnology* **20**, 434012 (2009).
- [9] A. Imamoglu *et al.*, *J. Appl. Phys.* **101**, 081602 (2007).
- [10] K. Hennessy *et al.*, *Nature (London)* **445**, 896 (2007).
- [11] M. Kaniber *et al.*, *Phys. Rev. B* **77**, 161303 (2008).
- [12] M. Winger *et al.*, *Phys. Rev. Lett.* **103**, 207403 (2009).
- [13] J. Suffczynski *et al.*, *Phys. Rev. Lett.* **103**, 027401 (2009).
- [14] N. Chauvin *et al.*, *Phys. Rev. B* **80**, 241306 (2009).
- [15] S. Ates *et al.*, *Nat. Photon.* **3**, 724 (2009).
- [16] A. Laucht *et al.*, *Phys. Rev. B* **81**, 241302 (2010).
- [17] A. Majumdar *et al.*, *Phys. Rev. B* **82**, 045306 (2010).
- [18] L. Besombes *et al.*, *Phys. Rev. B* **63**, 155307 (2001).
- [19] A. Berthelot *et al.*, *Nature Phys.* **2**, 759 (2006).
- [20] G. Tarel and V. Savona, *Phys. Rev. B* **81**, 075305 (2010).
- [21] U. Hohenester *et al.*, *Phys. Rev. B* **80**, 201311 (2009).
- [22] A. Auffèves, J. M. Gerard, and J. P. Poizat, *Phys. Rev. A* **79**, 053838 (2009).
- [23] K. Karrai *et al.*, *Nature (London)* **427**, 135 (2004).
- [24] E. I. Rashba, *Sov. Phys. Solid State* **2**, 1109 (1960).
- [25] M. H. Baier *et al.*, *Appl. Phys. Lett.* **84**, 648 (2004).
- [26] P. Gallo *et al.*, *Appl. Phys. Lett.* **92**, 263101 (2008).
- [27] M. Felici *et al.*, *Small* **5**, 938 (2009).
- [28] A. Mohan *et al.*, *Small* **6**, 1268 (2010).
- [29] R. Oulton *et al.*, *Opt. Express* **15**, 17 221 (2007).
- [30] D. Dalacu *et al.*, *Phys. Rev. B* **82**, 033301 (2010).
- [31] M. J. Hartmann, *Phys. Rev. Lett.* **104**, 113601 (2010).
- [32] R. Raussendorf and H. J. Briegel, *Phys. Rev. Lett.* **86**, 5188 (2001).
- [33] A. Mohan *et al.*, *Nat. Photon.* **4**, 302 (2010).
- [34] S. Hughes *et al.*, *Phys. Rev. B* **83**, 165313 (2011).